Hydrogen Bond Structure and Dynamics in Aqueous Electrolytes at Ambient and Supercritical Conditions

Elvira Guàrdia,*,† Daniel Laria,‡ and Jordi Martí†

Departament de Física i Enginyeria Nuclear, Universitat Politècnica de Catalunya, B4-B5 Campus Nord UPC, 08034 Barcelona, Catalonia, Spain, Unidad Actividad Química, Comisión Nacional de Energía Atómica, Av. del Libertador 8250, 1429 Buenos Aires, Argentina, and Departamento de Química Inorgánica, Analítica y Química Física, Facultad de Ciencias Exactas y Naturales, Universidad de Buenos Aires, Pabellón II, 1428 Buenos Aires, Argentina

Received: December 1, 2005; In Final Form: January 31, 2006

Hydrogen bond (HB) connectivity in aqueous electrolyte solutions at ambient and supercritical conditions has been investigated by molecular dynamics techniques. Alkali metal and halides with different sizes have been considered. Modifications in the water HB architecture are more noticeable in the first ionic solvation shells and do not persist beyond the second shells. The coordination pattern is established between partners located in the first and second solvation shells. High-temperature results show dramatic reductions in the coordination number of water; at liquidlike densities the number of HBs is close to 2, while in steamlike environments water monomers are predominant. The addition of ions does not bring important modifications in the original HB structure for pure water. From the dynamical side, the lifetime of HBs shows minor modifications due to the simultaneous competing effects from a weaker HB structure combined with a slower reorientational dynamics of water induced by the Coulomb coupling with solute. At supercritical conditions, the overall dynamics of HB is roughly 1 order of magnitude faster than that at ambient conditions, regardless of the particular density considered.

I. Introduction

Most of the peculiar properties that make water a unique fluid in nature are undoubtedly connected to its microscopic hydrogen-bond (HB) structure.[1,2] In the course of the last 50 years, the analysis of the nature of HB environments in water has drawn considerable interest, from both experimental and theoretical perspectives. However, despite these efforts, the subject still presents some controversies. Apparently simple questions, such as the gross features of the connectivity pattern in pure water, have been recently subjected to debate, since new results from X-ray absorption spectroscopy and X-ray Raman scattering[3] experiments would suggest *unexpected* asymmetries in water donor/acceptor characters. Moreover, the experimental evidence would bring the number of strong HBs down to values ∼2, clashing with the standard 4-fold coordination picture described in text books.

Ionic solvation introduces important modifications in the original intermolecular connectivity pattern that prevails in the pure solvent. From a structural perspective, the gross features of the effects of incorporating ionic species are normally described in terms of either stiffer or weaker HB structures. These concepts have been invoked to rationalize the observed thermodynamic quantities pertaining to the ionic solvation—most notably, solvation entropy—and the modification of transport properties of aqueous electrolytes as well. Anyhow, recent information from femtosecond pump−probe[4] and X-ray[5] experiments would show that the magnitude of these effects on the local water structure is, in reality, less important than previously thought and does not extend much farther than the first ionic solvation shell. From the dynamical side, the picture resulting from these studies suggests that overall HB dynamics slows down considerably compared to the pure water case.[6] The subject of this paper is intimately connected with these issues, since we focused attention on equilibrium and dynamical aspects of HB between this set of water molecules located in the close vicinity of ionic species.

HBs in aqueous electrolytes have been studied by a large variety of experimental techniques. To quote just of a few of them, the list includes: electric field,[7] calorimetric,[8] conductivity,[9] infrared and Raman spectroscopic measurements,[10−12] extended X-ray absorption fine structure spectroscopy,[13,14] neutron diffraction with isotopic substitution,[15−17] and, as we mentioned in the previous paragraph, nonlinear femtosecond spectroscopy.[6] On the theoretical side, computer simulations stand perhaps as the most valuable tool to analyze the structural and dynamical properties of ionic aqueous solutions at ambient,[18,19] high-temperature,[20−24] and supercritical states.[25−34] Hydrogen bonding has been investigated thoroughly, and estimates for average lifetimes of HBs have been obtained for water at different thermodynamic conditions,[35−39] at interfaces,[40,41] in aqueous electrolyte solutions,[42,43] and in systems of biological interest as well.[44] In an effort to provide a comprehensive description of the characteristics of HBs in close vicinity of ionic species, we present results from extensive molecular dynamics simulations, covering a wide variety of infinite diluted ionic species at ambient conditions. In addition, we explored thermal effects on the HB connectivity by considering supercritical ionic solutions as well.

* Corresponding author. E-mail address: elvira.guardia@upc.edu.
† Departament de Física i Enginyeria Nuclear, Universitat Politècnica de Catalunya.
‡ Unidad Actividad Química, Comisión Nacional de Energía Atómica and Departamento de Química Inorgánica, Analítica y Química Física, Facultad de Ciencias Exactas y Naturales, Universidad de Buenos Aires.

10.1021/jp056981p CCC: $33.50
Published on Web 03/08/2006

TABLE 1: Lennard-Jones Parameters for Ion−Water Interactions

ion	ϵ (kcal/mol)	σ (Å)	q (e)
Li^+	0.1600	2.336	1
Na^+	0.1245	2.875	1
K^+	0.1245	3.249	1
Cs^+	0.1245	3.525	1
F^-	0.1670	3.142	−1
Cl^-	0.1245	3.784	−1
I^-	0.1245	4.167	−1

The paper is organized as follows: in section II, we present details of the simulation procedure that we implemented. Section III includes the results for equilibrium characteristics of HBs. In section IV, dynamical aspects of HBs are described. The concluding remarks are presented in section V.

II. Computational Details and Hydrogen Bond Definition

A. Potential Models and Simulation Characteristics. We carried out molecular dynamics simulations at ambient conditions (T = 298 K, ρ = 1 g cm^{-3}) for several aqueous electrolytes. The list of ions included four alkali metal (Li^+, Na^+, K^+, Cs^+) and three halide (F^-, Cl^-, I^-) species. In addition, we also simulated aqueous Na^+ and Cl^- solutions at supercritical conditions. For the latter cases, the thermodynamic states were chosen along the T = 650 K isotherm, covering a range of solvent densities intermediate between ρ = 0.7 g cm^{-3} and ρ = 0.05 g cm^{-3}.

The SPC/E model[45] was chosen to model water−water interactions. The molecular dipole moment of SPC/E water is μ = 2.35 D, and its critical point is located approximately at T_c = 640 K, ρ_c = 0.29 g cm^{-3}.[46] This thermodynamic state is reasonably close to the experimental critical point of pure water, i.e., T_c = 647.13 K, ρ_c = 0.322 g cm^{-3}. The SPC/E model has been thoroughly tested in a variety of aqueous environments, including high-temperature states.[47−49] Ion−water interactions have been modeled as sums of Coulombic and 6-12 Lennard-Jones potentials terms. Energy and length parameters in the latter potential are displayed in Table 1. They have been obtained using the usual Lorentz−Berthelot rules applied to the set of parameters reported by Dang and co-workers.[50−53]

The time step in all simulation runs was set to 2 fs. In the case of aqueous electrolytes at room temperature, the experiments included initial equilibration runs of ∼50 ps, followed by simulation runs of typically ∼250 ps used to collect statistically meaningful properties. The simulations at supercritical conditions included initial stabilization runs somewhat longer, ∼100−250 ps, followed by production runs of approximately 0.5 ns. The simulated systems consisted of a single ion coupled to 255 water molecules contained in a cubic, periodically replicated, simulation box. In addition, auxiliary simulations of pure water at the same thermodynamic conditions were also performed. In these cases, the number of water molecules was set to 256 and the simulation lengths ranged from 50 up to 100 ps. Short-ranged forces were truncated at half the box length and the Ewald summation method was introduced to account for long-ranged, Coulomb interactions. Furthermore, we coupled the system to a Berendsen thermostat[54] in order to obtain an adequate temperature control.

B. Hydrogen-Bond Definition. We focused attention exclusively on hydrogen bond connectivity between water partners in aqueous solutions. The starting point of our analysis was the consideration of the water−water radial distribution functions; these functions were used as a guidance to establish reasonable definitions of H-bonding at ambient and supercritical conditions.

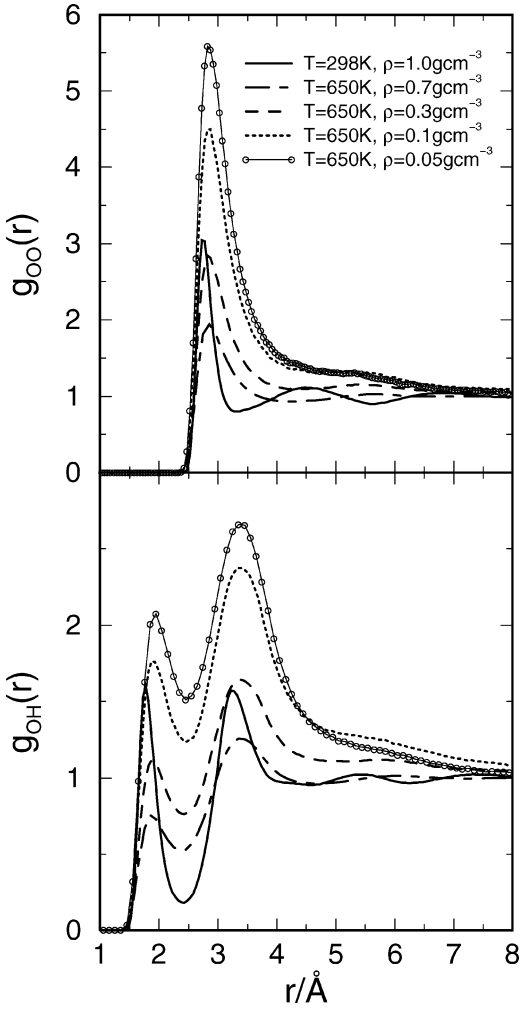

Figure 1. Oxygen−oxygen (top) and oxygen−hydrogen (bottom) radial distribution functions for pure water at different thermodynamic conditions.

It was assumed that two water molecules were H-bonded if the next three geometrical conditions were fulfilled:

(1) The distance R_{OO} between the oxygens remains smaller than R^c_{OO},

(2) The distance R_{OH} between the "acceptor" oxygen and the hydrogen "donor" atoms is smaller than R^c_{OH},

(3) The H−O···O angle φ is lower than φ^c. The threshold distances, R^c, were obtained from the corresponding first minima of the radial distribution functions $g_{OO}(r)$ and $g_{OH}(r)$ (see Figure 1). R^c_{OO} was set to 3.4 and 4.0 Å for ambient conditions and for for supercritical states, respectively. On the other hand, R^c_{OH} = 2.4 Å for all cases, regardless the particular temperature and/or density considered. The angular cutoff was chosen to be φ^c = 30°. This geometric definition has been found to be more adequate to describe intermolecular bonding in supercritical environments than alternative energetic criteria.[37]

III. Equilibrium Structure of Hydrogen Bonds

A. Room Temperature. The incorporation of ionic species in aqueous environments normally produces important modifications in spatial and orientational correlations of water. These changes are usually translated into modifications in the structure and dynamics of hydrogen bonds and their origins can be traced back to complex interplays between ion−water and water−water interactions. Of course, in infinite dilute solutions, these effects should gradually dissappear as we move away from the ion.

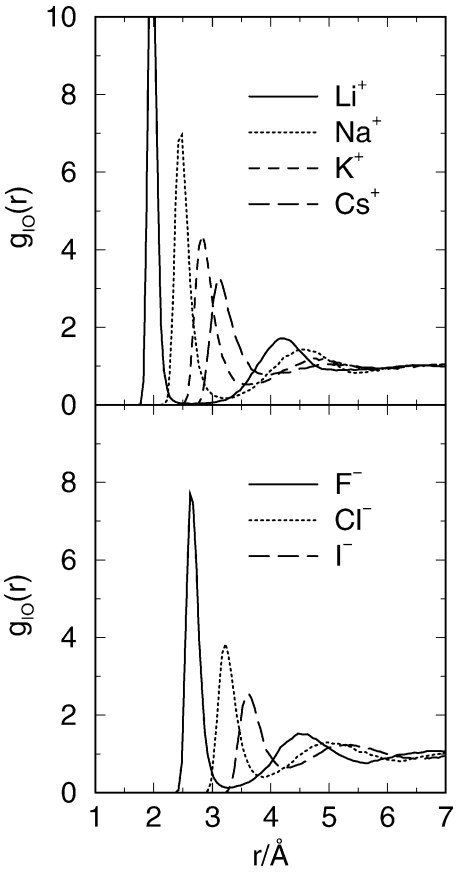

Figure 2. Ion−oxygen radial distribution functions for alkali metal (top) and halides (bottom) at $T = 298$ K and $\rho = 1$ g cm^{-3}.

TABLE 2: Hydration Shell Boundaries (R_{sh}), Shell Populations, (n_{sh}), and Percentage of HBs (P_j) between One Water Molecule Lying in the First Hydration Shell and a Second One Lying in the j Shell ($j = 1, 2$)'

ion	shell	R_{sh} (Å)	n_{sh}	P_1	P_2
Li^+	first	2.5	4	0.1	99
	second	5.0	14.5		
Na^+	first	3.2	6	2	95
	second	5.4	17		
K^+	first	3.6	7	9	87
	second	5.8	20		
Cs^+	first	4.0	9	17	74
	second	6.0	20		
F^-	first	3.2	6	1	97
	second	5.5	18		
Cl^-	first	3.8	7	2	96
	second	6.2	25		
I^-	first	4.2	7.5	3	93
	second	6.5	28		

To discriminate different local environments in the close vicinity of ionic species, we found it convenient to first analyze solute−solvent spatial correlations, as reflected by some relevant site−site pair correlation functions. The results are displayed in Figure 2. The locations of the first and second minima of these functions define the solvation shell boundaries for the variety of ionic solutes considered. Note that, as a general trend, first minima are unambiguously defined, but some uncertainties arise concerning the position of the second minimum for the largest cation considered, Cs^+. Full details of shell boundaries, R_{sh}, and shell populations, n_{sh}, are listed in Table 2.

The next step was the consideration of hydrogen bond connectivity within each particular solvation shell. To that end, we computed n_{HB}, the average number of hydrogen bonds per molecule, and the distributions p_n, namely the percentage of water molecules lying in the first and second solvation shells, that participate in n HBs. Results for the average values and distributions appear in Table 3. General qualitative trends can be readily perceived from the inspection of these entries:

TABLE 3: Percentages of Molecules (p_n) Forming $n = 1$, ..., 5 Hydrogen Bonds and Mean Number of HBs per Molecule (n_{HB}) in Aqueous Solutions at $T = 298$ K and $\rho = 1$ g cm^{-3}

ion	shell	p_0	p_1	p_2	p_3	p_4	p_5	n_{HB}
Li^+	first	1.1	17.0	65.2	16.5	0.2	0.0	1.97
	second	0.0	1.0	9.2	33.1	50.5	6.0	3.52
Na^+	first	1.3	13.9	43.9	38.8	2.1	0.0	2.27
	second	0.0	1.0	8.7	32.2	51.1	7.0	3.55
K^+	first	0.7	8.0	31.6	51.4	8.1	0.2	2.59
	second	0.0	0.9	8.5	32.6	51.4	6.4	3.54
Cs^+	first	0.0	4.0	21.4	52.7	20.8	0.9	2.92
	second	0.0	0.9	8.0	32.2	52.3	6.5	3.56
F^-	first	0.3	7.5	35.3	51.5	5.3	0.1	2.54
	second	0.0	0.9	8.6	33.0	51.4	6.1	3.53
Cl^-	first	0.2	5.7	31.8	54.0	8.1	0.3	2.65
	second	0.0	1.0	9.0	33.7	51.0	5.2	3.51
I^-	first	0.2	5.2	31.4	55.9	7.1	0.3	2.65
	second	0.0	1.0	9.4	34.1	50.3	5.1	3.50
H_2O		0.0	0.9	9.1	33.4	51.3	5.2	3.51

(i) As expected, changes in the HB connectivity (with respect to the neat water reference case) are more marked in the first ionic coordination shell, where n_{HB} (ninth column) are always smaller, regardless the nature and size of the ionic species considered. Of course, there is an obvious reason to account for the reduction of, at least, one hydrogen bond: Imagine replacing one water molecule in bulk water by an ion of similar size. For ions of type X^-, water molecules lying in the first solvation shell will very likely have one of their hydrogen atoms exhibiting a connectivity pattern of the type O−H···X^-. This simple argument seems to be enough to explain the overall reduction in $\Delta n_{HB} \sim -1$ for all anionic sizes. Conversely, for the cation cases, the presence of a nearby ion will exclude the possibility of a second water molecule to act as an eventual HB donor to the tagged water molecule.

(ii) On the other hand, changes are more marked for alkali metal solutes, where the deficit may reach $\Delta n_{HB} \sim -1.5$ for the Li^+ case.

(iii) Effects from the presence of the ionic solutes on hydrogen bonding seem to fade away already in the second solvation shell, at least from the simplest perspective of counting HB and the corresponding distributions p_n. Note that the overall characteristics of the water−water connectivity resemble very much the one prevailing in pure water. This conclusion seems accordant with results from pump−probe spectroscopy experiments performed on aqueous $Mg(ClO_4)_2$, reported by Omta et al.[4]

To gain further insight into the characteristics of the intermolecular connectivity pattern in the close vicinity of ionic species, we also computed P_j, the percentage of hydrogen bonds established between one water molecule lying in the first solvation shell and a second one lying in the j shell ($j = 1, 2$). Results for P_j, are listed in Table 2. The physical picture that emerges from these results suggests the following: (i) Leaving aside for the moment the particular case of Cs^+, hydrogen bond connectivity for water molecules lying within the first solvation shell is exclusively established with molecules located in the outer, second shell. (ii) For the case of anions, they act as single donors and accept an average of ∼1.5 HBs from neighboring partners. (iii) For the case of cations, the scenario is somewhat different and the connectivity depends on the ionic size considered. For small size ions, such as the Li^+ case, water molecules in the first solvation shell normally act exclusively as double donors of HBs. However, as the solute size increases,

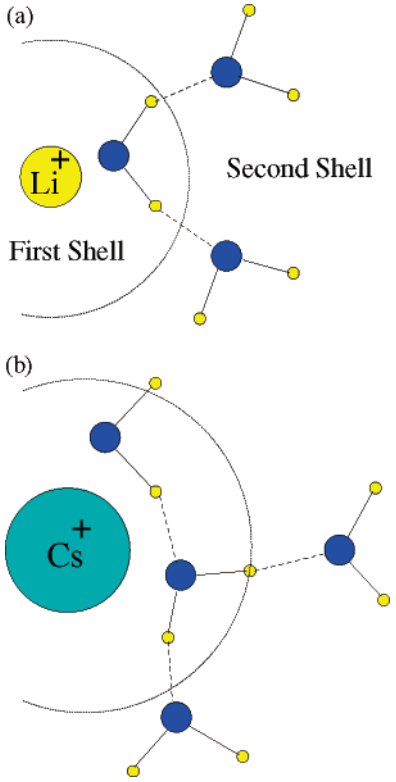

Figure 3. HB connectivity patterns for water molecules in the first solvation shell of alkali-metal ions of different sizes: (a) small size; (b) large size.

they may develop a single acceptor character as well. The pictures shown in Figure 3 are cartoons corresponding to the hydrogen bond connectivity patterns described in the previous lines. In passing, we remark that for Cs^+ the reduction in the ion−water coupling, due to the larger size of the ion, allows a percentage of 17% of molecules that are H-bonded with partners within the same first solvation shell.

B. Supercritical States. Oxygen-ion radial distribution functions computed at several densities along the $T = 650$ K isotherm are presented in Figure 4. For Na^+, we observe that both first and second hydration shells are located at practically the same positions for all densities, whereas for Cl^- the positions of the first minima tend to shift toward larger distances as density decreases. Similar features have been previously observed in neutron diffraction experiments[17] and in computer simulations[30] as well. For the sake of completeness, shell populations and boundaries are listed in the fourth and fifth columns of Table 4.

Results for the statistics of HB in supercritical ionic solutions, expressed in terms of the density dependence of n_{HB}, are presented in Figure 5 and also listed in Table 4. As a reference benchmark, we have also included results for pure water. First, we remark the important changes operated on the n_{HB} for pure water at $T = 650$ K. At typical liquid densities, thermal effects lead to a drastic drop of practically ca. two hydrogen bonds per molecule. Moreover, a subsequent reduction in density shifts the latter values down to the ones for practically monomeric structures, namely, $n_{HB} \sim 0.3$. In the presence of ionic species, density effects in the water−water connectivity become somewhat milder: For the first ionic shell, n_{HB} varies typically from ∼1.4−1.2 at $\rho = 0.7$ g cm^{-3} down to ∼0.65−0.75 at $\rho = 0.05$ g cm^{-3}. Inspection of the entries in the last three columns of Table 4 show that for Na^+, the connectivity pattern of HB is the same at all densities and involves mainly partners lying in

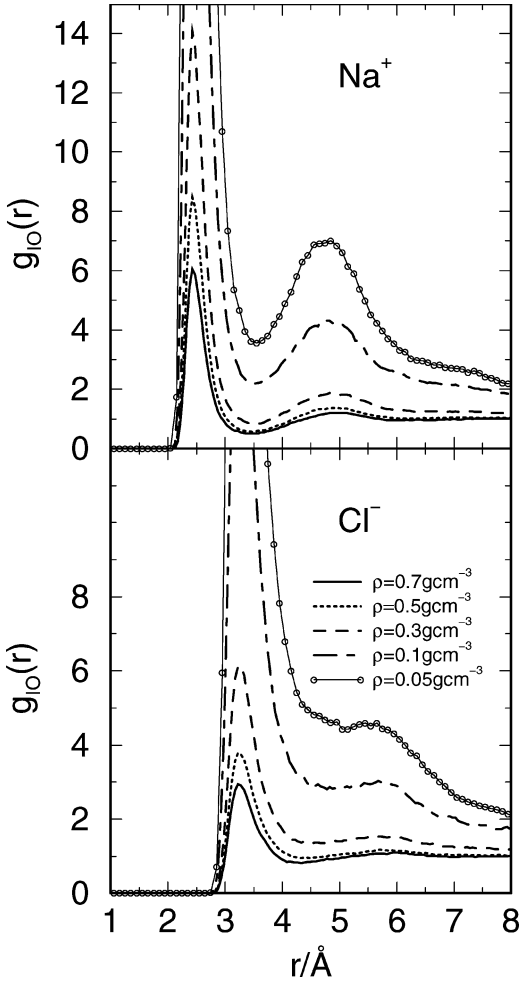

Figure 4. Ion−oxygen radial distribution functions for Na^+ (top) and Cl^- (bottom) dissolved in supercritical water at different densities.

TABLE 4: Hydration Shell Boundaries (R_{sh}), Shell Populations, (n_{sh}), Average Number of HBs (n_{HB}), and Percentages of HB (P_j) between One Water Molecule Lying in the First Hydration Shell and a Second One Lying in the j Shell ($j = 1, 2$) for Supercritical Aqueous Na^+ and Cl^-

ion	ρ (g cm^{-3})	shell	R_{sh} (Å)	n_{sh}	n_{HB}	P_1	P_2
Na^+	0.7	first	3.5	6	1.3	9	90
		second	6.0	17	1.9		
	0.5	first	3.5	5.5	1.1	9	90
		second	6.0	13.5	1.6		
	0.3	first	3.5	5.5	1.0	9	90
		second	6.0	11.0	1.5		
	0.1	first	3.5	5.0	0.8	9	90
		second	6.0	8.0	1.3		
	0.05	first	3.5	5.0	0.7	9	90
		second	6.0	6.0	1.0		
Cl^-	0.7	first	4.2	7.5	1.5	13	86
		second	7.0	26.0	1.8		
	0.5	first	4.5	8.0	1.3	20	78
		second	7.0	19.0	1.6		
	0.3	first	4.5	7.5	1.1	21	77
		second	7.0	15.0	1.4		
	0.1	first	4.6	7.0	0.9	26	74
		second	7.2	10.5	1.0		
	0.05	first	5.0	7.0	0.8	38	61
		second	7.5	7.0	0.9		

the first and second solvation shells ($P_2 \sim 90\%$). This observation should be contrasted with the case of Cl^- where, as we move down toward steamlike densities, there is a steady growth of P_1 (from ∼10% up to ∼40%), in detriment of P_2. More interesting perhaps is the fact, that a similar analysis performed

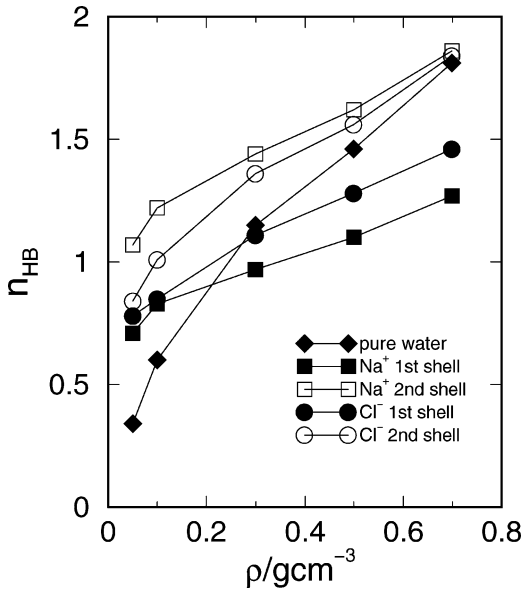

Figure 5. Average number of HBs per molecule in the close vicinity of ionic species dissolved in supercritical water. Also shown are the results for the pure solvent. In all cases error bars are of similar magnitude to the symbol sizes.

in the second solvation shell shows a larger degree of water−water connectivity compared to the one found for the first solvation shell. The conclusions drawn from these observations can be summarized as follows: (i) The enhancement of the local water density in the vicinity of the ion at low densities—which is mainly the results of the strong Coulombic coupling between neighboring water molecules and the ion—benefits the possibility of a higher extent of HB connectivity, compared to the pure water case. (ii) We tend to believe that the reasons why HB connectivity in the second shell is higher, compared to that prevailing in the first shell, are to be found in the, normally competing, water−ion and water−water interactions, already mentioned in previous paragraphs. Should this line of reasoning be correct, molecules in the second shell would be less tightly coupled to the ionic electric field and could modify their orientational degrees of freedom to promote a more efficient intermolecular connectivity with their partners at a relative, smaller, energy cost.

IV. Hydrogen Bond Dynamics

A. Room Temperature. To investigate the dynamics of the HB network in all electrolyte solutions, we resorted on analysis of a relevant set of time correlation functions. Briefly, a variable η_{ij}, associated with the connectivity state between the molecular pair (i, j) was defined according to the following convention:[55,56]

$$\eta_{ij}(t) = 1, \quad \text{if molecules } i \text{ and } j \text{ form an HB at times 0 and } t, \text{ and the bond has not been broken for any period longer than } t^*$$
$$\eta_{ij}(t) = 0, \quad \text{otherwise} \tag{1}$$

The threshold time interval t^* will be defined below. In this context, it is useful to define a normalized HB lifetime autocorrelation function $C_{HB}(t)$ defined as

$$C_{HB}(t) \equiv \sum_{i,j} \frac{\langle \eta_{ij}(0)\, \eta_{ij}(t) \rangle_{t^*}}{\langle \eta_{ij}{}^2(0) \rangle_{t^*}} \tag{2}$$

TABLE 5: Continuous (τ_{HB}^{cont}) and Intermittent (τ_{HB}^{int}) Integrated H-bond Lifetimes for Aqueous Solutions at Ambient Conditions. Also Shown Are Relevant Orientational and Residence Characteristic Times (see text)

				τ_α^{reor} (ps)			
ion	shell	τ_{HB}^{cont} (ps)	τ_{HB}^{int} (ps)	$\mathbf{u}_\mu$	$\mathbf{u}_{OH}$	$\mathbf{u}_{HH}$	τ_{res} (ps)
Li^+	first	0.52	4.5	15.9	6.7	4.8	101
	second	0.53	4.2	4.9	4.6	4.4	10.5
Na^+	first	0.44	3.5	7.1	4.8	4.0	25.0
	second	0.51	3.6	4.4	4.3	4.3	9.2
K^+	first	0.48	3.6	4.7	4.4	4.3	8.2
	second	0.53	4.0	4.5	4.5	4.5	6.8
Cs^+	first	0.53	3.8	4.9	4.6	4.5	6.9
	second	0.54	3.8	4.7	4.6	4.6	6.3
F^-	first	0.55	4.7	7.7	9.9	11.2	35.5
	second	0.54	4.2	4.7	4.7	4.7	11.0
Cl^-	first	0.56	4.6	6.0	6.2	6.3	14.0
	second	0.55	4.2	5.1	4.7	4.5	10.2
I^-	first	0.57	4.2	5.7	4.9	4.6	8.5
	second	0.56	4.1	4.8	4.6	4.5	9.2
H_2O		0.54	3.9	4.4	4.2	4.2	

where $\langle ... \rangle_{t^*}$ represents a time average that depends on the choice for t^*. Two limiting cases have been considered: (*i*) $t^* = 0$, which represents the so-called continuous approximation for the lifetime (C_{HB}^{cont}), i.e., no bond breakings and consequent reformations in the time interval [0, t], and (*ii*) $t^* = \infty$, which corresponds to the case of intermittent hydrogen bonds (C_{HB}^{int}) which persist at time t, regardless multiple breaking and reformation processes in the course of its previous temporal history. The main features of these time correlation functions have been extensively analyzed in previous studies.[38,40,41,43] Perhaps the most important conclusion that can be drawn is the fact that the long time decay of C_{HB}^{int} presents nonexponential kinetics.[38] Moreover, the variety of time scales governing the decay of C_{HB}^{int} is the result of the coupling that exists between the HB population and diffusional modes.

Table 5 contains results for τ_{HB}^{int} and τ_{HB}^{con}, the integrated continuous and intermittent correlation times, respectively. For completeness, we have also computed average residence times of water in each solvation shell[57] and three relevant reorientational characteristic times, obtained from time integrals of correlations of the type

$$\tau_\alpha^{reor} = \int_0^\infty \langle \boldsymbol{u}_\alpha(t) \cdot \boldsymbol{u}_\alpha(0) \rangle \, dt \tag{3}$$

where $\mathbf{u}_\alpha = \hat{\mu}$ and $\hat{\mathbf{r}}_{OH}$ and $\hat{\mathbf{r}}_{HH}$ correspond to unit vectors along the directions of the water dipole moment, the OH and the HH intramolecular bonds, respectively.

Several observations concerning the entries of Table 5 are in order. Although the differences are not dramatic, there seems to be clear evidence that the HB dynamics for water lying in the neighborhood of cations presents a nonmonotonic size dependence. Note that for the Na^+ case, continuous and intermittent time scales are the shortest. As a reasonable argument to rationalize this feature, we can speculate about subtle cancellations between two competing effects, both originated in the electric field generated by the solute. We are referring to (i) the overall slower rotational dynamics of water (see the three entries for τ_α^{reor} for small size solutes) thwarted by (ii) the distorted and energetically weakened, water structure in the close vicinity of the ion. On the other hand, for the anionic species, the former effects seem to prevail for all sizes considered, since the tendency is uniform; i.e., the larger the solutes (and, consequently, the weaker the ionic coupling with water), the smaller the corresponding time scale. It should also

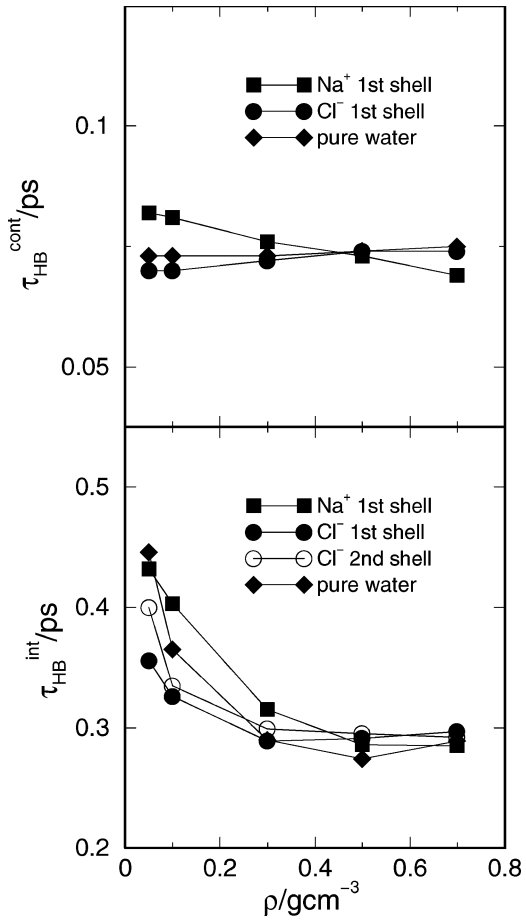

Figure 6. HB continuous (top panel) and intermittent (bottom panel) lifetimes for water molecules lying in the close vicinity of ionic species at supercritical conditions. Also shown are the results for the pure solvent. In all cases error bars are of similar magnitude to the symbol sizes.

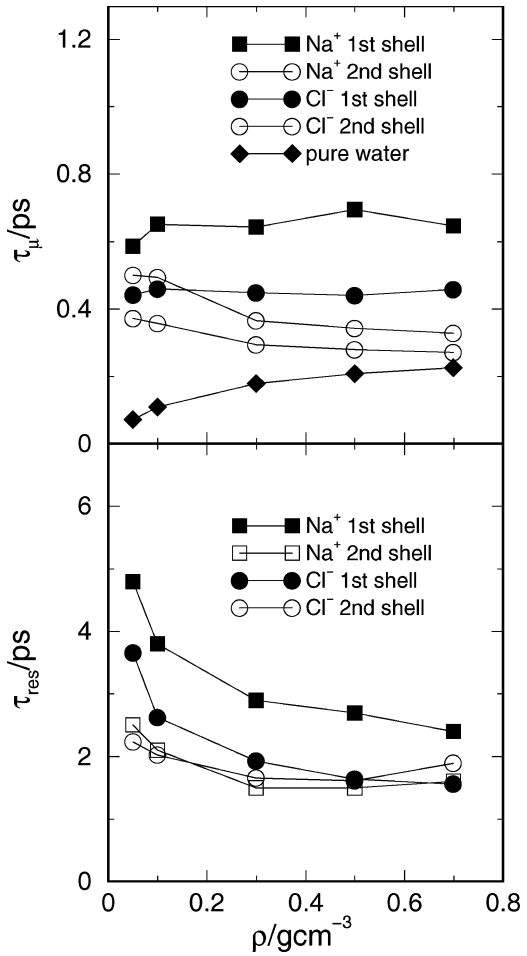

Figure 7. Same as Figure 6 for the characteristic dipole−dipole orientational correlation time (top panel) and residence time (bottom panel).

be noted that, except for the already mentioned Na^+ result, the HB dynamics for water in second solvation shells are practically identical to those found for the pure liquid. Finally, we point out that the magnitude of water residence times in both solvation shells is in all cases at least a factor of 2 larger than the characteristic times describing the intermittent HB. Consequently, we tend to believe that effects from translational modes arising from mutual diffusion on the dynamics of HB between a tagged pair of water molecules should be much less important than those operating in pure water.

B. Dynamics of HB at Supercritical Conditions. The last aspect to be investigated deals with thermal and density effects on the dynamics of HB for aqueous electrolytes at supercritical conditions. Results for τ_{HB}^{cont} and τ_{HB}^{int} for water in the vicinity of infinite diluted Na^+ and Cl^- are depicted in the top and bottom panels of Figure 6. As expected, one observes that temperature effects lead to drastic reductions (roughly, 1 order of magnitude) of the characteristic times. The passage from liquidlike down to steamlike environments produces barely perceptible changes in τ_{HB}^{cont} and a mild slowing down of the intermittent HB dynamics. Besides, at a first glance, all distinctive characteristics originated in size and charge sign of the solutes are of difficult detection; moreover, note that the Coulombic ion−water coupling seems to have little effect on the dynamics of HB, since all τ_{HB} values for the pure solvent fall within the dispersion of the results for ionic species.

To get additional clues about the observed density and temperature effects on the dynamics, it will be useful to reexamine the time scales describing orientational correlations and residence times for water at high temperatures that are shown in Figure 7. The faster overall orientational dynamics in the subpicosecond time domain, as reflected by τ_{μ},[58] could in principle account for the observed results for τ_{HB}^{cont}, since the lifetime of a continuous HB is normally driven by fast rotational and librational modes. On the other hand, it is interesting to note that lifetimes of intermittent HB present a density trend qualitatively similar to that observed for the residence times which, in turn, are dependent on interdiffusive modes. In this respect, the characteristics of the intermittent dynamics would preserve—although with a sensible reduction—some of the distinctive features that characterize HB dynamics of water at ambient conditions. We finally would like to point out that the drastic reduction in the average of n_{HB} to values, in many cases, below unity are likely to affect the accuracy of the statistics in a nonnegligible fashion. As such, our conclusions in this respect still await additional and more conclusive confirmation.

V. Concluding Remarks

We have carried out extensive molecular dynamics simulations of aqueous alkali metal and halides at ambient and supercritical conditions in order to explore the effects of ionic size, charge sign, temperature, and density on the intermolecular connectivity of water in the close vicinity of these solutes. At ambient conditions, perhaps the most important result of this paper is the validation of the experimental evidence[4,5] suggesting that the modifications in HB connectivity do not extend beyond

the first solvation shell. The presence of the solute induces a coordination reduction which is more noticeable in solvation shells of small cations. This coordination is mostly established between partners located in the first and second solvation shells, although for the largest cation investigated (Cs^+) we did observe a sizable fraction of HB between partners both lying in the first solvation shell.

As expected, a rise in temperature also produces important changes in the HB network. Typical values of n_{HB} move down to practically ~2 at high densities, while in steamlike environments, the drop is even more dramatic, with clear prevalence of water monomers. In the latter circumstances, further addition of ionic species does promote a nonnegligible degree of water clustering around the solute; however, these changes do not translate into important modifications in the water−water connectivity.

From a dynamical perspective, the most relevant feature is that the lifetimes of HB do not seem to be affected in a sensible fashion by the presence of ions. We tend to believe that this is the result of competing effects originated in (i) a weaker HB structure (an accelerating factor) compensated by (ii) the Coulomb coupling with solute, which slows down the reorentational dynamics of neighboring water molecules. In all cases, the larger residence times observed would lead to a more effective decoupling between the HB dynamics and diffusional modes. Concerning thermal effects on the dynamics, all supercritical time scales present drastic reductions, while subsequent reductions in density seem to affect the characteristic time scales only mildly.

Acknowledgment. The authors gratefully acknowledge financial support from the Secretaría de Educación y Universidades de España, the Direcció General de Recerca de la Generalitat de Catalunya (Grant 2001SGR-00222) and the Ministerio de Educación y Ciencia de España (Grant BFM2003-08211-C03-01). Additional funding by the European Union FEDER funds (UNPC-E015) is also acknowledged. D.L. is a member of Carrera del Investigador Científico de CONICET (Argentina).

References and Notes

(1) Eisenberg, D.; Kauzmann, W. *The Structure and Properties of Water*; Oxford University Press: New York, 1969.

(2) *Water*: *A Comprehensive Treatise*; Franks, F., Ed.; Plenum Press: New York, 1972.

(3) Wermet, P.; Nordlund, D.; Bermann, U.; Cavallieri, M.; Odeliu, M.; Ogasawara, H.; Näslund, L. A.; Hirsch, T. K.; Ojamäe, L.; Glatzel, P. Petterson, L. G. M.; Nilsson, A. *Science* **2004**, *304*, 995.

(4) Omta, A. W.; Kropman, M. F.; Woutersen, S.; Bakker, H. J. *Science* **2003**, *301*, 347. Omta, A. W.; Kropman, M. F.; Woutersen, S.; Bakker, H. J. *J. Chem. Phys.* **2003**, *119*, 12457.

(5) Näslund, L.-A.; Edwards, D. C.; Wernet, P.; Bergmann, W.; Ogasawara, H.; Pettersson, L. G. M.; Myneni, S.; Nilsson, A. *J. Phys. Chem. A* **2005**, *109*, 5995.

(6) Kropman, M. F.; Nienhuys, H.-K.; Bakker, H. J. *Phys. Rev. Lett.* **2002**, *88*, 077601. Kropman, M. F.; Bakker, H. J. *Science* **2001**, *291*, 2118. Kropman, M. F.; Bakker, H. J. *J. Chem. Phys.* **2001**, *115*, 8942.

(7) Mesmer, R. E.; Sweeton, F. H.; Hitch, B. F.; Baes, C. F. In *High-temperature High-Pressure Electrochemistry in Aqueous Solutions*; Jones, D. d. G., Staehle, R. W., Eds.; National Association of Corrosion Engineers: Houston, TX, 1976; pp 365−374.

(8) Wood, R. H.; Smith-Magowan, D. In *Thermodynamics of Aqueous Systems with Industrial Applications*; Newman, S. A., Ed.; American Chemical Society: Washington, DC, 1980; Vol. 133, pp 569−581.

(9) Marshall, W. L.; Frantz, J. D. In *Hydrothermal Experimental Techniques*; Ulmer, G. C., Barnes, H. L., Eds.; John Wiley and Sons: New York, 1987; Chapter 11.

(10) Walrafen, G. E. *J. Chem. Phys.* **1966**, *44*, 1546.

(11) Walrafen, G. E. *J. Chem. Phys.* **1970**, *52*, 4176.

(12) Amo, Y.; Tominaga, Y. *Physica A* **2000**, *275*, 33.

(13) Pfund, D. M.; Darab, J. G.; Fulton, J. L.; Ma, Y. *J. Phys. Chem.* **1994**, *98*, 13102.

(14) Wallen, S. L.; Pfund, D. M.; Fulton, J. L. *J. Chem. Phys.* **1998**, *108*, 4039.

(15) Enderby, J. E. *Chem. Soc. Rev.* **1995**, *24*, 159.

(16) de Jong, P. H. K.; Neilson, G. W.; Bellissent-Funel, M. C. *J. Chem. Phys.* **1996**, *105*, 5155.

(17) Yamaguchi, T.; Yamagami, M.; Ohzono, H.; Wakita, H.; Yamanaka, K. *Chem. Phys. Lett.* **1996**, *252*, 317.

(18) Koneshan, S.; Rasaiah, J. C.; Lynden-Bell, R. M.; Lee, S. H. *J. Phys. Chem. B* **1998**, *102*, 4193.

(19) Chowdhuri, S.; Chandra, A. *J. Chem. Phys.* **2001**, *115*, 3732.

(20) Chialvo, A. A.; Cummings, P. T.; Simonson, J. M.; Mesmer, R. E. *J. Chem. Phys.* **1999**, *110*, 1064.

(21) Chialvo, A. A.; Cummings, P. T.; Simonson, J. M.; Mesmer, R. E. *J. Chem. Phys.* **1999**, *110*, 1075.

(22) Driesner, T.; Cummings, P. T. *J. Chem. Phys.* **1999**, *111*, 5141.

(23) Lee, S. H.; Cummings, P. T. *J. Chem. Phys.* **2000**, *112*, 864.

(24) Chialvo, A. A.; Kusalik, P. T.; Cummings, P. T.; Simonson, J. M. *J. Chem. Phys.* **2001**, *114*, 3575.

(25) For recent review articles on computer simulation of water and aqueous ionic solutions at supercritical conditions, see: Kalinichev, A. G. *Rev. Mineral. Geochem.* **2001**, *42*, 83. Chialvo, A. A.; Cummings, P. T. *Adv. Chem. Phys.* **1999**, *109*, 105.

(26) Balbuena, P. B.; Johnston, K. P.; Rossky, P. J. *J. Phys. Chem.* **1996**, *100*, 2706.

(27) Lee, S. H.; Rasaiah, J. C. *J. Phys. Chem.* **1996**, *100*, 1420.

(28) Balbuena, P. B.; Johnston, K. P.; Rossky, P. J.; Hyun, J.-K. *J. Phys. Chem. B* **1998**, *102*, 3806.

(29) Koneshan, S.; Rasaiah, J. C. *J. Chem. Phys.* **2000**, *113*, 8125.

(30) Rasaiah, J. C.; Noworyta, J. P.; Koneshan, S. *J. Am. Chem. Soc.* **2000**, *122*, 11182.

(31) Noworyta, J. P.; Koneshan, S.; Rasaiah, J. C. *J. Am. Chem. Soc.* **2000**, *122*, 11194.

(32) Koneshan, S.; Rasaiah, J. C.; Dang, L. X. *J. Chem. Phys.* **2001**, *114*, 7544.

(33) Hyun, J.-K.; Johnston, K. P.; Rossky, P. J. *J. Phys. Chem. B* **2001**, *105*, 9302.

(34) Masia, M.; Rey, R. *J. Phys. Chem. B* **2003**, *107*, 2651.

(35) Mizan, T. I.; Savage, P. E.; Ziff, R. M. *J. Phys. Chem.* **1996**, *100*, 403.

(36) Martí, J.; Padró, J. A.; Guàrdia, E. *J. Chem. Phys.* **1996**, *105*, 639.

(37) Martí, J. *J. Chem. Phys.* **1999**, *110*, 6876.

(38) Luzar, A.; Chandler, D. *Nature* (*London*) **1996**, *379*, 55. Luzar, A.; Chandler, D. *Phys. Rev. Lett.* **1996**, *76*, 928. Luzar, A. *J. Chem. Phys.* **2000**, *113*, 10663.

(39) Martí, J. *Phys. Rev. E* **2000**, *61*, 449.

(40) Paul, S.; Chandra, A. *Chem. Phys. Lett.* **2004**, *386*, 218.

(41) Liu, P.; Harder, E.; Berne, B. J. *J. Phys. Chem. B* **2005**, *109*, 2949.

(42) Chandra, A. *Phys. Rev. Lett.* **2000**, *85*, 768.

(43) Chandra, A. *J. Phys. Chem. B* **2003**, *107*, 3899.

(44) Balasubramanian, S.; Pal, S.; Bagchi, B. *Phys. Rev. Lett.* **2002**, *89*, 115501.

(45) Berendsen, H. J. C.; Grigera, J. R.; Straatsma, T. P. *J. Phys. Chem.* **1987**, *91*, 6269.

(46) Guillot, B.; Guissani, Y. *J. Chem. Phys.* **1993**, *98*, 8221.

(47) Bellissent-Funel, M. C.; Tassaing, T.; Zao, H.; Beysens, D.; Guillot, B.; Guissani, Y. *J. Chem. Phys.* **1997**, *107*, 2942.

(48) Rønne, C.; Thrane, L.; Åstrand, P. O.; Wallqvist, A.; Mikkelsen, K. V.; Keiding, S. R. *J. Chem. Phys.* **1997**, *107*, 5319.

(49) Guàrdia, E.; Martí, J. *Phys. Rev. E* **2004**, *69*, 011502.

(50) Dang, L. X. *J. Chem. Phys.* **1992** *96*, 6970.

(51) Dang, L. X.; Garrett, B. C. *J. Chem. Phys.* **1993**, *99*, 2972.

(52) Smith, D. E.; Dang, L. X. *J. Chem. Phys.* **1994**, *100*, 3757.

(53) Dang, L. X. *J. Am. Chem. Soc.* **1995**, *117*, 6954.

(54) Berendsen, H. J. C.; Postma, J. P. M.; van Gunsteren, W. F.; Di Nola, A.; Haak, J. R. *J. Phys. Chem.* **1984**, *81*, 3684.

(55) Rapaport, D. C. *Mol. Phys.* **1983**, *50*, 1151.

(56) Padró, J. A.; Saiz, L.; Guàrdia, E. *J. Mol. Struct.* **1997**, *416*, 243.

(57) For calculation procedures of residence times, see: Impey, R. W.; Madden, P. A.; McDonald, I. R. *J. Phys. Chem.* **1983**, *87*, 5071. In all cases, we have used $t^* = \infty$.

(58) For a more comprehensive analysis of orientational dynamics in aqueous supercritical ambients, see: Guàrdia, E.; Laria, D.; Martí, J. *J. Mol. Liq.*, in press. (doi: 10.1016/j.molliq.2005.11.028)